High Efficiency n-Type Emitter-Wrap-Through Silicon Solar Cells

Fabian Kiefer, Christian Ulzhöfer, Till Brendemühl, Nils-Peter Harder, Rolf Brendel, Verena Mertens, Stefan Bordihn, Christina Peters, and Jörg W. Müller

***Abstract*—In the ALBA-II project, Q-Cells SE, Bitterfeld-Wolfen, Germany, and the Institute for Solar Energy Research Hamelin, Emmerthal, Germany, are developing high-efficiency emitter-wrap-through (EWT) solar cells on n-type silicon wafers. N-type silicon grown by the Czochralski (Cz) method forms the basis of this high-efficiency solar cell development as it offers high bulk carrier lifetimes. The EWT device structure allows us to employ a simplified process sequence compared with interdigitated back-contact back-junction solar cells. High open-circuit voltages of our solar cells are achieved by different passivation layers for base and emitter surfaces and picosecond laser ablated contact openings. An optimization of the resistances along the current paths in base and emitter leads to an improvement in fill factor *(FF)* over former EWT solar cells. Together with the inherently high current densities of EWT solar cells, we achieve on our small-area (4-cm^2, designated area without busbars) cells a short-circuit current density J_{SC} of 40.4 mA/cm^2, an open-circuit voltage V_{OC} of 661 mV, *FFs* well above 80%, and, thus, cell efficiencies of up to 21.6%.**

***Index Terms*—Emitter-wrap-through (EWT), n-type silicon, silicon solar cells.**

I. Introduction

WITHIN the ALBA-II project, Q-Cells, Bitterfeld-Wolfen, Germany, and the Institute for Solar Energy Research Hamelin (ISFH), Emmerthal, Germany, are developing high-efficiency emitter-wrap-through (EWT) solar cells for n-type silicon wafers. The EWT solar cell was originally proposed as a technique to accomplish high efficiency, even for rather low-quality absorber material [1]. The large coverage of electrically interconnected emitter areas at the front and rear sides of the cell allows us to collect high current densities in this cell structure with no need for high bulk lifetimes. However, one finds in practice that low fill factor (*FF*) values make the cell efficiency to lag behind those expectable from short-circuit current density J_{SC} and open-circuit voltage V_{OC} values. This effect cannot be understood in terms of ohmic power dissipation within the EWT vias. Instead, a recombination enhancement caused by lateral current flows is responsible for reducing the *FF* and efficiency, particularly for relatively high wafer resistivities higher than 3 Ω·cm and lower quality material [2]. Furthermore, this effect can be increased by a high via-resistivity [3]. For that reason, we propose also to use n-type Czochralski (Cz) silicon material with a resistivity of 1.5 Ω·cm and high carrier lifetimes for EWT cells instead of the commonly used boron-doped p-type Cz–Si which suffers from strong recombination due to boron–oxygen complexes [4]. Back-contacted high-efficiency solar cell concepts on n-type silicon typically employ three different diffusion processes to create three differently doped surface regions of the device: front-surface field (FSF), back-surface field (BSF), and emitter [5], [6]. The device architecture of EWT solar cells allows us employing heavier doped front surfaces than those required for efficient FSF structures. Thus, in EWT solar cells, one can simplify the cell process sequence compared with the process of an interdigitated back-contact back-junction (IBC-BJ) solar cell. One can avoid one high-temperature step and combine the preparation of the front and rear emitter in a single diffusion process [7]. The high surface doping concentration of the front-emitter diffusion diminishes the influence of the front-surface passivation quality. More importantly, the recombination associated with the relatively heavy emitter diffusion does not compromise the J_{SC} current collection significantly, as opposed to back-junction IBC solar cells. One result is that the *I–V* characteristics of a high-efficiency EWT solar cell are more robust against variations in front passivation quality and bulk lifetime compared with back-junction solar cells. This robustness against variations leads to a more reliable cell performance.

We achieve high open-circuit voltages by passivating the front and rear boron-diffused p-type emitter by a stack of aluminum oxide and silicon nitride (Al_2O_3-SiN_x) [8], [9] (drawn in blue in the cross section in Fig. 1). In order to avoid current transport losses by the majority carriers in the solar cell volume, we include a $POCl_3$-diffusion process that forms a BSF (red in Fig. 1). This lowers the total base resistance and, connected with this, the voltage drop inside the bulk material. A similar observation was published in [10] for the influence of an FSF

Manuscript received July 13, 2011; revised August 1, 2011; accepted August 2, 2011. Date of publication September 29, 2011; date of current version October 27, 2011. This work was supported by the German Federal Ministry for the Environment, Nature Conservation and Nuclear Safety, under Contract 0329988C (ALBA II).

F. Kiefer and T. Brendemühl are with the Institute for Solar Energy Research Hamelin, 31860 Emmerthal, Germany (e-mail: kiefer@isfh.de; brendemuehl@isfh.de).

C. Ulzhöfer was with the Institute for Solar Energy Research Hamelin, 31860 Emmerthal, Germany. He is now with SMT Maschinen und Vertriebs GmbH & Co. KG, 97877 Wertheim, Germany (e-mail: christian.ulzhoefer@web.de).

N.-P. Harder is with the Institute for Solar Energy Research Hamelin, 31860 Emmerthal, Germany, and also with the Institute of Electronic Materials and Devices, University of Hanover, 30167 Hanover, Germany (e-mail: harder@isfh.de).

R. Brendel is with the Institute for Solar Energy Research Hamelin, 31860 Emmerthal, Germany, also with Institute of Solid State Physics, University of Hanover, 30167 Hanover, Germany (e-mail: brendel@isfh.de).

V. Mertens, S. Bordihn, C. Peters, and J. W. Müller are with Q-Cells SE, 06766 Bitterfeld-Wolfen, Germany (e-mail: v.mertens@q-cells.com; st.bordihn@q-cells.com; c.peters@q-cells.com; j.mueller@q-cells.com).

Color versions of one or more of the figures in this paper are available online at http://ieeexplore.ieee.org.

Digital Object Identifier 10.1109/JPHOTOV.2011.2164953

2156-3381/$26.00 © 2011 IEEE

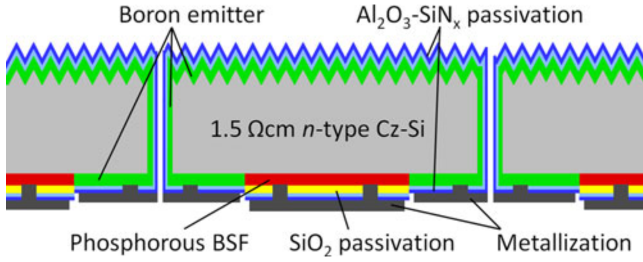

Fig. 1. Schematic cross section of the EWT solar cell (not to scale).

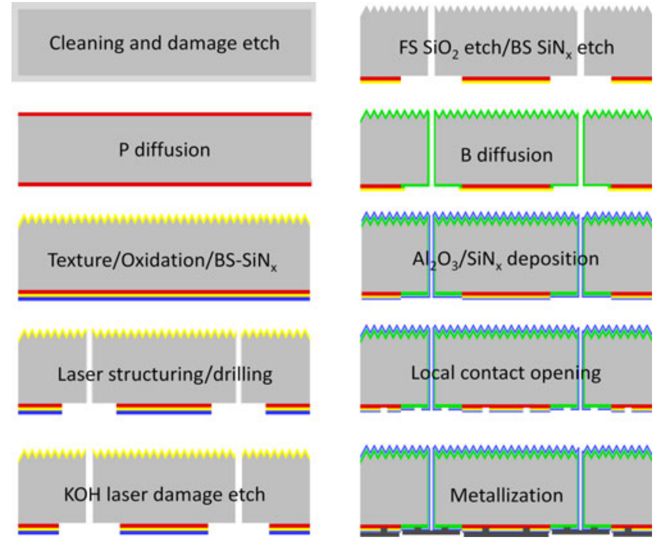

Fig. 2. Process sequence of the ALBA EWT solar cell.

in back-junction solar cells. The resulting decrease in recombination leads to an increase in the *FF*. We passivate the BSF by a thermally grown silicon dioxide (SiO_2; yellow in Fig. 1), which gets covered during the subsequent cell process by the Al_2O_3-SiN_x passivation stack.

II. Experimental Details

We present an EWT solar cell process that comprises two diffusion steps, alongside with an additional oxidation at high temperature. Fig. 1 shows a schematic of the cross section of these cells. The solar cell process includes

1) a phosphorous diffusion providing a BSF;
2) a thermal oxidation that drives in the phosphorous profile and grows a silicon dioxide. The silicon dioxide is used as a passivation layer for the BSF;
3) a boron diffusion creating a 50-Ω/□ emitter, without the formation of a boron-rich layer (BRL).

We passivate the boron-diffused emitter of our n-type cells with an aluminum oxide-silicon nitride stack that results in saturation current densities J_0 lower than 60 fA/cm^2 on textured and on planar emitter surfaces, respectively. The silicon-dioxide-passivated BSF surface exhibits J_0 values of 120 fA/cm^2. The local contacts through the passivation layers for emitter and base are created by picosecond laser ablation [11]. We use evaporated aluminum for metalizing the rear side of the solar cell. A short summary of the process sequence and the schematic cross section of the cell are depicted in Fig. 2.

A. Front Side

We use a BBr_3 open-tube boron diffusion process for preparing a p-type emitter with a sheet resistance of 50 Ω/□. The same process is used to form the emitter inside the EWT vias.

Boron diffusions achieving high lifetimes can be conducted at high temperatures up to 960 °C [12]. We choose to perform the boron diffusion process at moderate temperatures below 900 °C in order to avoid the formation of a BRL during the diffusion process. As a result, any potential for BRL-induced carrier lifetime degradation is completely avoided [13].

Fig. 3(a) shows data from the injection dependent lifetime measurement of a boron-diffused reference sample with an aluminum oxide silicon nitride passivation made from the same material as the solar cells. The Al_2O_3-SiN_x-passivated emitter shows saturation current densities of 60 or 40 fA/cm^2 on textured or planar surfaces, respectively. The values have been

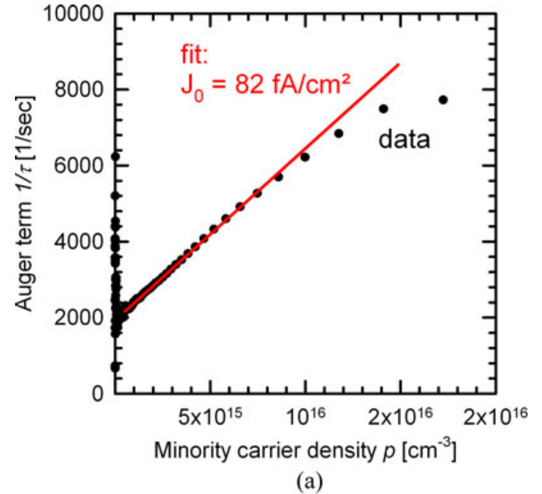

(a)

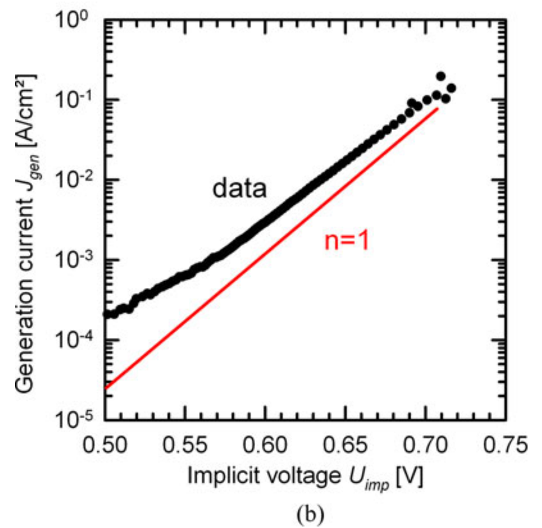

(b)

Fig. 3. Carrier lifetime measurement of a boron-diffused and Al_2O_3-passivated n-type Cz silicon wafer with planar surface. (a) Inverse lifetime versus minority carrier density. (b) Implicit *I–V* curve of the sample.

extracted with the method proposed in [14]. Low J_0 values of the boron-diffused surfaces are an important prerequisite for achieving high V_{OC} values. Note that in EWT solar cells, almost all surfaces are covered by the emitter, which is the entire front side and about 50% of the rear side. According to ray-tracing simulations made with Sunrays [15], the optical properties of the Al_2O_3-SiN_x stack are comparable with an SiN_x single-layer, despite of the nonideal change in refractive indices: There is nearly no difference in reflection and absorption behavior of both front-side layer configurations, if the Al_2O_3 layer is sufficiently thin, i.e., below 20 nm.

Fig. 3(b) depicts the implied *I–V* curve calculated from the effective lifetime data. These data show that the recombination properties of our boron diffusion produce only a marginal reduction of the *FF.* The ideality factor of the implied *I–V* curve is close to unity and approaches a value of 1 for voltages above 0.55 V, i.e., at the bias levels of the 1-sun maximum power point of our solar cell.

B. Rear Side

Most EWT solar cells report so far only *FFs* below 79% [7], [16], which, in most cases, overcompensated the positive influence of high currents, compared with front- or back-junction solar cells. It is, therefore, important to carefully design the current transport paths within an EWT cell. The reasons for these comparatively low *FFs* of EWT solar cells are pronounced series resistances and voltage drops along the current paths in the solar cell, causing enhanced resistive and recombination losses along these paths [2]. Both the bulk minorities (by the long emitter current paths, where they are the majority carriers) and the bulk majorities (by lateral current flow) contribute to this effect. The voltage drop along the emitter path is of same importance as the voltage drop due to the resistivity of the base volume. To attenuate the effect of the lateral bulk majority carrier transport, we implement a BSF to our 1.5-Ω·cm base, which reduces the lateral voltage drop inside the base by a lower overall base resistance. Fig. 4 shows the simulation results of a 3-D simulation of the majority carrier current flow in the base. The symmetry element is similar to the cell presented in this paper. The via distance is 500 μm, and the index accounts 1400 μm (1000 μm for the experimental cells) with a rear-side emitter coverage of 50%. The simulation covers the case of a cell with a BSF [see Fig. 4(a)] and a cell without a BSF [see Fig. 4(b)]. The simulations were carried out with the same SENTAURUS simulation model as described in [2]. In case of a BSF, the majorities predominantly flow within the highly conductive BSF, whereas the absence of a BSF requires long transport paths through the lowly conducting base. The differences in base conductance between the two cases are as follows.

BSF [see Fig. 4(a)] and non-BSF [see Fig. 4(b)] cause different magnitudes of quasi-Fermi level (QFL) potential drops along the majority carrier transport paths. In particular, at the point farthest from the base contact, the QFL potential drop is much more pronounced in the case of the absence of a BSF [see Fig. 4(b)]. Note that the QFL can be identified with the voltage drop inside the base volume and is, therefore, indicative of the

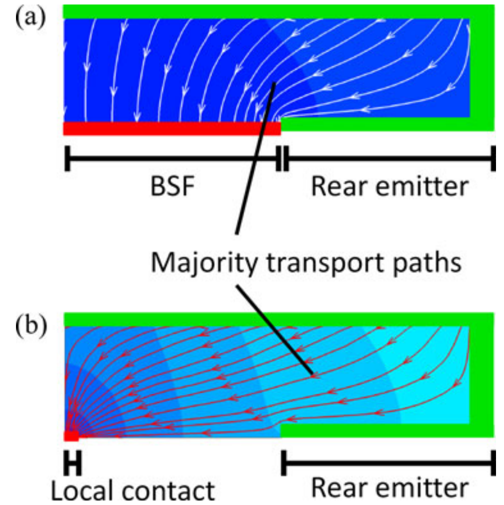

Fig. 4. Simulation of the majority transport paths and the QFLs in the symmetry element of an EWT solar cell with base resistivity of 0.8 Ω·cm. Dark blue indicates a ΔQFL of 0 mV and light blue a ΔQFL of 6 mV. Simulation graphs are taken from [17]. (a) *BSF case*: The majorities flow into the high conducting BSF, and the QFL at the farthest point is 1 mV higher than at the base contact. (b) *Non-BSF case*: The majority of the carriers flow through the base into the base contact, and the QFL at the farthest point from the base contact is raised by 6 mV.

series resistance losses. We find that even in case of a highly conducting base with resistivity of 0.8 Ω·cm, the difference between the BSF and the non-BSF case accounts for about 5 mV. We simulate an *FF* decrease of $0.4\%_{\mathrm{abs}}$ [17].

In addition, the highly doped surface of the BSF decreases the resistance of the base contact. We passivate the BSF surfaces by a thermally grown silicon oxide, which also serves as an effective dielectric mirror at the solar cell rear side. The SiO_2-passivated BSF achieves J_0 values of about 130 fA/cm^2.

Due to the high lifetime bulk material and the well-passivated surfaces, there is only a small base recombination current density, and the QFL can be assumed as nearly constant. This allows us to estimate a total saturation current density of the entire solar cell by adding up the J_0 values of the surfaces with respect to their surface area fraction. The calculated total J_0 of 200 fA/cm^2 corresponds well with the measured open-circuit voltage of 661 mV.

We also prepared reference EWT solar cells, where the entire noncontacted rear-side area – that is, the emitter and the BSF– was covered with the Al_2O_3-SiN_x passivation stack which is used for the boron emitter. However, we find that the cells with the oxidized BSF layer exhibit significantly higher V_{OC} values, exceeding those of the cells without oxidation by about 30 mV. It is known that the passivation quality of an Al_2O_3-SiN_x layer on a phosphorous diffused surface is lower compared with an SiO_2 layer. Nevertheless, measured surface recombination current densities on lifetime samples with the same surface preparation can explain only a 5-mV lower open-circuit voltage. The reason for this extraordinarily high loss in V_{OC} has yet to be found and is still under investigation.

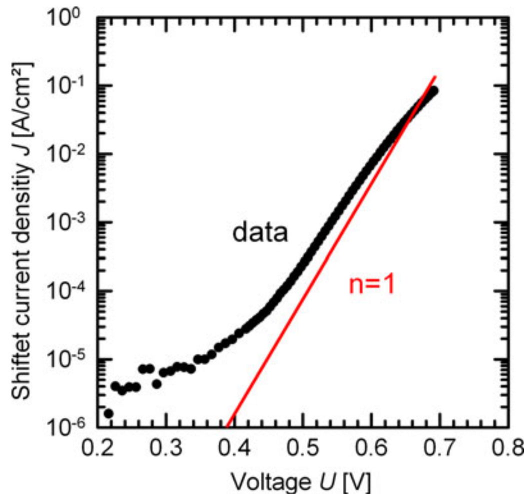

Fig. 5. J_{SC}-shifted *I–V* curve of the best cell exhibiting nearly ideal recombination (ideality factor close to unity) for the relevant operation voltages higher than 0.45 V.

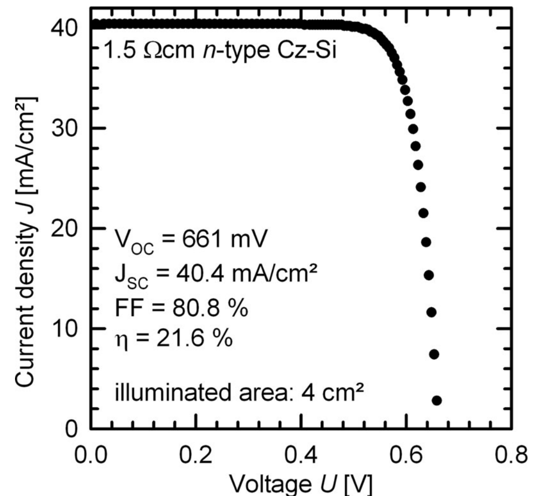

Fig. 6. *I–V* curve of the best cell, measured on 4-cm^2 designated area without busbars.

C. Emitter Vias

For the preparation of the EWT vias in the laser-drilled holes, we apply the same boron diffusion that we use for the preparation of our 50-Ω/□ boron-doped emitter on the front and rear sides of the cell. In this process, we obtain a higher emitter sheet resistance inside the EWT vias. Three-dimensional simulations of the symmetry element were carried out to determine the voltage drop between the front-side emitter and the contacted rear-side emitter of the solar cell. The EWT-via conductivity was calculated to be sufficient to achieve *FFs* above 80%. However, the low-resistance front-side emitter has to be traded against a loss in blue response of the front-side emitter, which lies in the range of 0.4 mA/cm^2 compared with a 75-Ω/□ emitter. This emitter sheet resistance would lead to a 1.5 times higher via conductivity for the chosen EWT index and via distance. This would lower the *FF* of the solar cell by about $1\%_{\mathrm{abs}}$.

A lower voltage drop along the whole emitter is also realized by the choice of a small index, i.e., the emitter and base fingers are 500 μm in width. Along with a via distance of 500 μm, the maximum path of an electron inside the front-side emitter is below 560 μm.

The optimized current paths in emitter and base lead to reduced transport losses and improved recombination behavior of the EWT solar cell as can be seen in the J_{SC}-shifted *I–V* curve of the cell in Fig. 5. We find nearly ideal recombination (ideality factor close to unity) above 0.45 V, resulting in a high *FF* of 80.8%.

D. Contact Openings

The openings on both the emitter and the BSF are made with a frequency doubled Nd:YVO_4-laser with a wavelength of 532 nm and pulse durations of about 10 ps [11], [18]. The area fraction of the openings was chosen to be 3%, which was calculated to be sufficient for low contact resistance. The contact openings on the back-side emitter are close to the vias with consideration of the emitter current paths.

The cell results in this paper indicate that picosecond laser ablation of Al_2O_3-SiN_x layers from boron-doped emitter surfaces neither leads to damage on the surfaces nor to shunts in the solar cell. The suitability of picosecond laser ablation of SiO_2 on phosphorous diffused silicon surfaces was shown in [19].

E. Cell Performance

The recombination behavior of our EWT solar cell was optimized in several ways. The resistivities of base and emitter were adjusted to diminish the voltage drop along the current paths of electrons and holes, which influences the ideality of recombination in the solar cell. A high and injection-independent lifetime of the n-type bulk volume and low J_0 values of the base and emitter surfaces also have a positive influence on the total saturation current of the solar cell. The ideality factor of the *I–V* curve is close to unity in a broad voltage range between 0.45 and 0.6 V. This resulted in an *FF* of 80.8%.

Different passivation stacks on base and emitter lead to an open-circuit voltage of up to 661 mV. The current collection in the EWT solar cells is high due to the double-side emitter coverage. The efficiency of the best cell was measured to be 21.6% with an illuminated area of 4 cm^2. This area includes only the finger structure of the EWT cell, without busbars. The *I–V* curve of the cell is depicted in Fig. 6.

III. Summary

We established a stable EWT solar cell process on n-type Czochralski grown silicon with in-house measured designated area (4 cm^2) efficiencies of 21.6%. We use n-type material to combine high carrier lifetimes with high bulk material conductivity. This allows us achieving high *FFs* for our EWT solar cells. The current paths and—along with this—the recombination behavior of the solar cell were designed to diminish charge carrier transport-induced losses, which resulted in high solar cell *FFs* up to 80.8%.

ACKNOWLEDGMENT

The authors would like to thank A. Lohse, N. Braun, and M. Berger for solar cell processing and the ISFH laser team for the assistance in laser processing.

REFERENCES

[1] J. M. Gee, W. Kent Schubert, and P. A. Basore, "Emitter wrap-through solar cell," in *Proc. 23rd IEEE Photovoltaic Spec. Conf.*, 1993, pp. 265–270.

[2] C. Ulzhöfer, P. P. Altermatt, N.-P. Harder, and R. Brendel, "Loss analysis of emitter-wrap-through silicon solar cells by means of experiment and three-dimensional device modeling," *J. Appl. Phys.*, vol. 107, pp. 104509-1–104509-12, 2010.

[3] C. Ulzhöfer, S. Hermann, N.-P. Harder, P. P. Altermatt, and R. Brendel, "VIRE-effect: Via-resistance induced recombination enhancement—The origin of reduced fill factors of emitter wrap through solar cells," in *Proc. 24th Eur. Photovoltaic Solar Energy Conf. Exh.*, 2009, pp. 937–941.

[4] J. Schmidt, A. G. Aberle, and R. Hezel, "Investigation of carrier lifetime instabilities in Cz grown silicon," in *Proc. 26th IEEE Photovoltaic Spec. Conf.*, 1997, pp. 13–18.

[5] F. Granek, C. Reichel, M. Hermle, D. M. Huljić, O. Schultz, and S. W. Glunz, "Front surface passivation of n-type high-efficiency back-junction silicon solar cells using front surface field," in *Proc. 22nd Eur. Photovoltaic Solar Energy Conf. Exh.*, 2007, pp. 1262–1265.

[6] W. Mulligan and R. Swanson, "High-efficiency, one-sun cell processing," in *Proc. 13th NREL Crystalline Silicon Workshop*, 2003, pp. 30–37.

[7] P. Engelhart, A. Teppe, A. Merkle, R. Grischke, R. Meyer, N.-P. Harder, and R. Brendel, "The RISE-EWT solar cell—A new approach towards simple high efficiency silicon solar cells," in *Proc. 15th Int. Photovoltaic Solar Energy Conf. Exh.*, 2005, pp. 802–803.

[8] B. Hoex, J. Schmidt, R. Bock, P. P. Altermatt, M. C. M. van de Sanden, and W. M. M. Kessels, "Excellent passivation of highly doped P-type Si surfaces by the negative-charged-dielectric Al_2O_3," *Appl. Phys. Lett.*, vol. 91, pp. 112107-1–112107-3, 2007.

[9] J. Schmidt, B. Veith, and R. Brendel, "Effective surface passivation of crystalline silicon using ultrathin Al_2O_3 films and Al_2O_3/SiN_X stacks," *Phys. Status Solidi RRL*, vol. 3, pp. 287–289, 2009.

[10] F. Granek, M. Hermle, D. M. Huljić, O. Schultz-Wittmann, and S. W. Glunz, "Enhanced lateral current transport via the front N^+ diffused layer of n-type high-efficiency back-junction back-contact silicon solar cells," *Prog. Photovoltaics Res. Appl.*, vol. 17, pp. 47–56, 2009.

[11] P. Engelhart, N.-P. Harder, T. Neubert, H. Plagwitz, B. Fischer, R. Meyer, and R. Brendel, "Laser processing of 22% efficient back-contacted silicon solar cells," in *Proc. 21st Eur. Photovoltaic Solar Energy Conf. Exh.*, 2006, pp. 773–776.

[12] A. Edler, J. Jourdan, V. D. Mihailetchi, R. Kopecek, R. Harney, D. Stichtenoth, T. Aichele, A. Grochocki, and J. Lossen, "High lifetime on n-type silicon wafers obtained after boron diffusion," in *Proc. 25th Eur. Photovoltaic Solar Energy Conf. Exh.*, 2010, pp. 1905–1907.

[13] M. A. Kessler, T. Ohrdes, B. Wolpensinger, and N.-P. Harder, "Charge carrier lifetime degradation in Cz silicon through the formation of a boron-rich-layer during BBr3 diffusion processes," *Semicond. Sci. Tech.*, vol. 25, pp. 055001-1–055001-9, 2010.

[14] D. E. Kane and R. M. Swanson, "Measurement of the emitter saturation current by a contactless photoconductivity decay method," in *Proc. 18th IEEE Photovoltaic Spec. Conf.*, 1985, pp. 578–583.

[15] R. Brendel, "Sunrays: A versatile ray tracing program for the photovoltaic community," in *Proc. 12th Photovoltaic Solar Energy Conf. Exh.*, 1994, pp. 1339–1342.

[16] D. Kray, J. Dicker, D. Osswald, A. Leimenstoll, S. W. Glunz, W. Zimmermann, K.-H. Tentscher, and G. Strobl, "Progress in high-efficiency emitter-wrap-through cells on medium quality substrates," in *Proc. 3rd World Conf. Photovoltaic Energy Convers.*, 2003, pp. 1340–1343.

[17] C. Ulzhöfer, Ph.D. dissertation, to be published.

[18] S. Hermann, N.-P. Harder, R. Brendel, D. Herzog, and H. Haferkamp, "Picosecond laser ablation of SiO_2 layers on silicon substrates," *Appl. Phys. A*, vol. 99, pp. 151–158, 2010.

[19] P. Engelhart, S. Hermann, T. Neubert, H. Plagwitz, R. Grischke, R. Meyer, U. Klug, A. Schoonderbeek, U. Stute, and R. Brendel, "Laser ablation of SiO_2 for locally contacted Si solar cells with ultra-short pulses," *Progr. Photovoltaics: Res. Appl.*, vol. 15, pp. 521–527, 2007.

Authors' photographs and biographies not available at the time of publication.